FRONT-SCAN SONAR USING SYNTHETIC APERTURE

F Mosca IXSEA SAS, La Ciotat, France
F Jean IXSEA SAS, La Ciotat, France

1 INTRODUCTION

SHADOWS is a towed-fish developed by IXSEA SAS, containing two high-performance side-scan sonar system imaging a six hundred meter swath at a resolution of 15cm (Fig.1).[1]

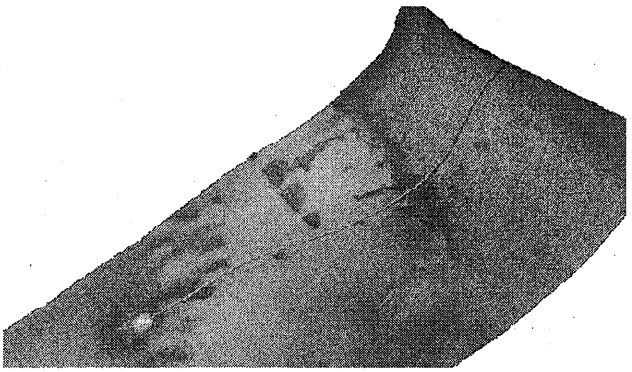

Fig. 1.View of a sewage pipe in La Ciotat bay (France) made with SHADOWS

The gap at the nadir of the towed-fish is around thirty meters. In order to image this gap, a GapFiller (GFS) is being developed. The aim of this system is to fulfill the blind area at nadir preserving the sonar image type with echoes/shadows contrast area. Thus this system is different from other GapFiller using multibeam sonar, indeed the kind of images obtained is no more depth and bathymetric data.

The insonified area (Fig.2) is forty-five meter large ($Y = 45m$) to ensure a good overlap with the side-scan data. The range projection on the sea-floor is between sixty and eighty meters ($60m < X < 80m$), to allow an eventual synthesis that we will discuss further. The height of the towed fish is about thirty meters ($H = 30m$).

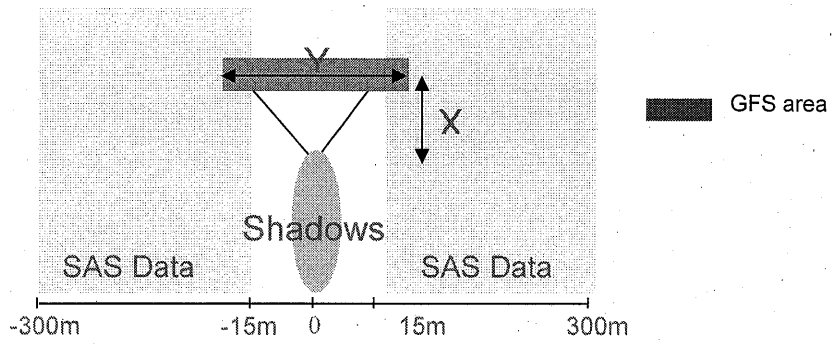

Fig. 2. Image area of the GFS

This system presents constraints for its implementation. First, the electronic of the towed fish is designed to manage forty-eight sensors ($N_{sen} \leq 48$) and four emission frequencies ($N_{em} = 4$).[2]
Moreover, in order to fit out the SHADOWS'towed-fish, the receiving array of the front-scan sonar must be less than 80 centimeters.
The main objective of the GFS is to image the gap in real-time with a quality close to the SAS images. The target resolution to reach is less than fifty centimeters.

2 CHARACTERISTICS AND PRINCIPLE

2.1 First choices

From the objectives set before, two consequences appear. First, the choice of the working frequency: the across-track resolution is:

$$\delta R = \frac{\lambda R}{L}$$

with λ the wavelength, R the range and L the length of the receiving array. Thus, with a small antenna (less than 80 centimeters), the only way to improve the resolution is to increase the frequency. A good compromise between the range of 80m and the resolution is a working frequency of 400 kHz.

The second choice for our system is to minimize the quantity of data by using an ambiguous antenna, in order to receive information from several directions with only one set of data. This ambiguity comes from the spatial under-sampling of a network antenna.

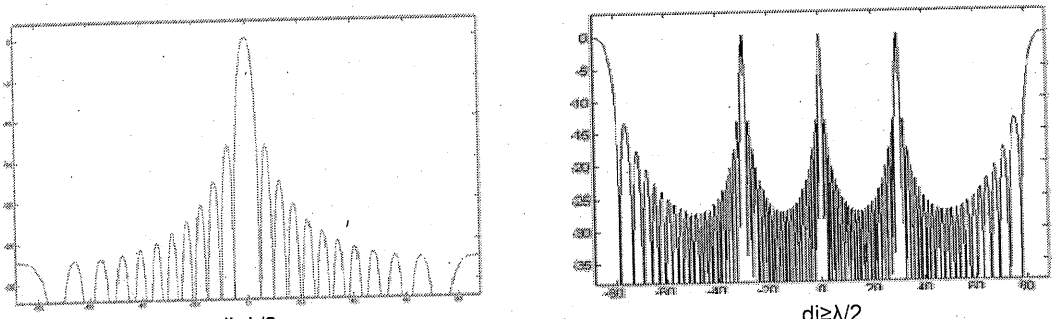

di≤λ/2
Non ambiguous antenna

di≥λ/2
Ambiguous antenna

Fig.3: Directivity pattern of an ambiguous and non ambiguous antenna

2.2 The sectorized emission principle

The ambiguous reception permits to reduce the amount of data but it introduces an ambiguity on the direction of reception during the beamforming. To suppress this ambiguity, the sectorized emission principle is used. It consists in using several emitters, in our case four, working at four different frequencies around the central frequency of 400 kHz.

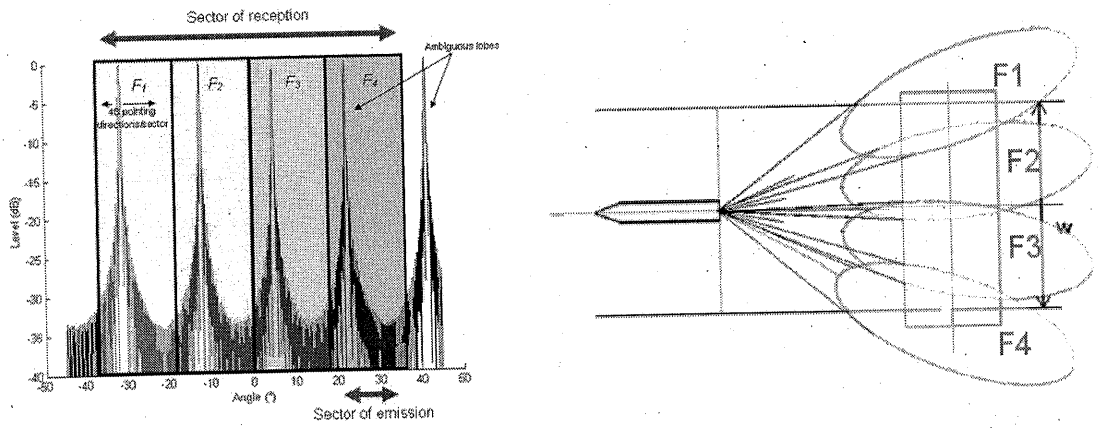

Fig.4: The sectorized emission principle pattern

3 CONTRAST

3.1 Definition

The combination of an ambiguous reception and a non-focalized emission induces a loss of the performance of the system in term of image quality. A good criterion to evaluate it is the level of contrast between bottom and shadow reverberation.
To define this level of contrast we use the sonar equation, where the reverberation level is:

$$RL = SL - 2TL + BR + DI_r + PG$$

And the level of shadow is:

$$OL = NL$$

With: SL : Source Level ; TL : Transmission Loss ; BR : Bottom Reverberation ; DI_r : Directivity Index in reception ; PG : Processing Gain ; NL : Noise Level
Thus the level of contrast is simply: $SL - 2TL + BR + DI_r + PG - NL$.

3.2 Secondary lobe contribution

In our case, the level of contrast will be smaller because the shadow is not infinite. This effect will be more visible for a small object in the lobe axis because we receive the reverberation energy in the secondary lobe of the reception array.

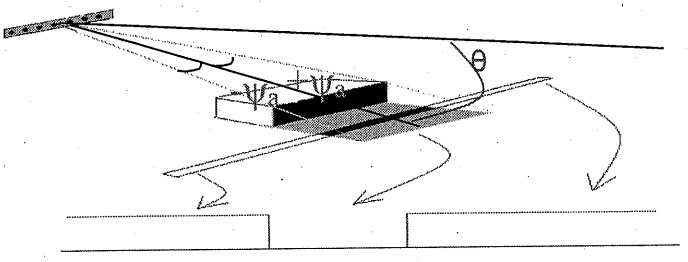

Fig.5: Geometry of the contrast evaluation

To estimate this phenomenon, we suppose a flat bottom at the angle θ from the horizontal. The instantaneous signal received from the range r corresponds to an horizontal surface: $\frac{c}{2B\cos\theta}$.
The level of the signal received from r is:

$$s(r) = \iint_{\theta,\psi} l(\psi,\theta) f(\psi,\theta,r) p(\theta,\psi) \cos\theta d\psi d\theta$$

With l the reverberation coefficient in the pointing direction, $f^2(\theta,\psi)$, the directivity function, $p(\theta,\psi)$, the pressure level in the direction (θ,ψ) (taking into account the transmission losses, the emission level and the directivity).
As the bottom is non-coherent, we can make a summation in energy in order to see the mean backscattered level:

$$\left\langle s^2(r) \right\rangle = \iint_{\psi,\theta} \left\langle l^2(\theta,\psi) \right\rangle f^2(\theta,\psi) p^2(\theta,\psi) \cos^2\theta d\theta d\psi$$

If we calculate the vertical directivity for a signal from r, we can see:

$$f_0^2(\theta) = 1 \text{ if } \theta \in \frac{c}{2B}\tan\theta_0$$

So finally the level of reverberation is:

$$\left\langle s^2(r)\right\rangle = \int_{-\psi_a}^{\psi_a} \left\langle l^2(\theta_0,\psi)\right\rangle f^2(\psi) p^2(\psi) \frac{c}{2B} \cos\theta_0 \sin\theta_0 d\psi$$

For a shadow, the integration is the same without the backscattering level in the pointing direction.
We can see on the figure 6 the echographic mode of the GFS and the importance of the secondary lobe contribution:

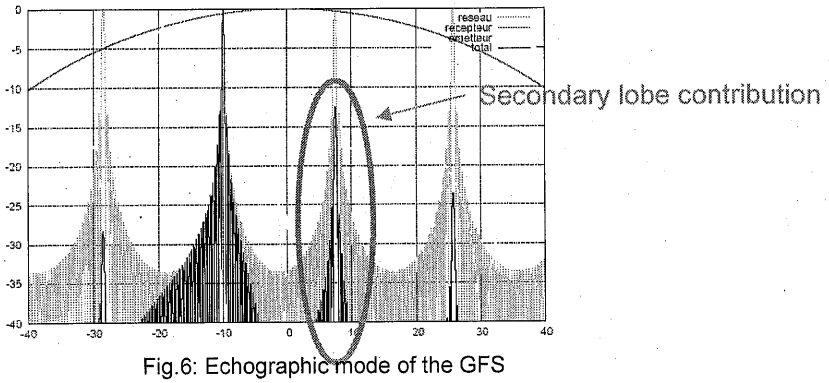

Fig.6: Echographic mode of the GFS

3.3 Expression of the contrast

Setting a size of shadow which is twice the sonar resolution: $\psi_a = 0.89\frac{c}{fn_r\delta_r}$, we can suppress the level in the totality of the main lobe. In this case, the equation is:

$$\left\langle n^2(r)\right\rangle = \left\langle s^2(r)\right\rangle - \int_{-\psi_a}^{\psi_a} \left\langle l^2(\theta_0,\psi)\right\rangle f^2(\psi) p^2(\psi) \frac{c}{2B} \cos\theta_0 \sin\theta_0 d\psi$$

Thus, the contrast is:

$$C = 10\log_{10}\left[1 - \frac{1}{\left\langle s^2(r)\right\rangle}\int_{-\psi_a}^{\psi_a} \left\langle l^2(\theta_0,\psi)\right\rangle f^2(\psi) p^2(\psi) \frac{c}{2B} \cos\theta_0 \sin\theta_0 d\psi\right]$$

4 TRANSDUCER PERFORMANCE

In order to validate our ceramic-block architecture some tests have been made on models in our test tank in Brest. Comparisons between finite element modelling and experimental results have been made (Fig.10 & 11) and we can notice a good agreement on sensitivity and directivity between finite element modelling and acoustic experiments all along the bandwidth.

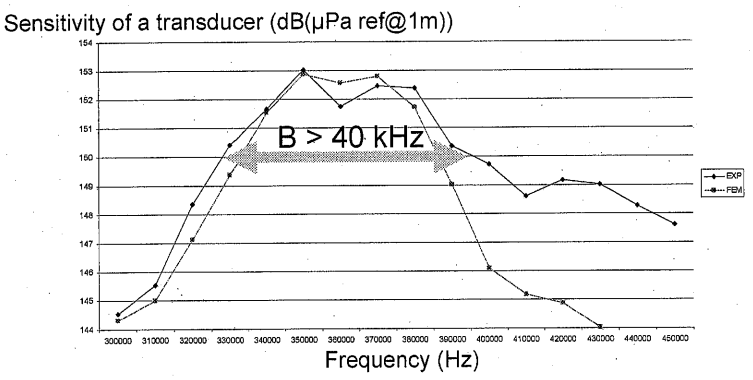

Fig.6: Comparison between FEM and the experiment

5 DIMENSION AND PERFORMANCE

5.1 Signal to noise ratio

We can read sensitivity in emission of our transducer is: $S_v = 153dB$. So the signal level for a supply of 600Vrms is: $SL = S_v + 20\log(V) = 208dB$.

So, using the sonar equation the signal to noise ratio varies with the range like:

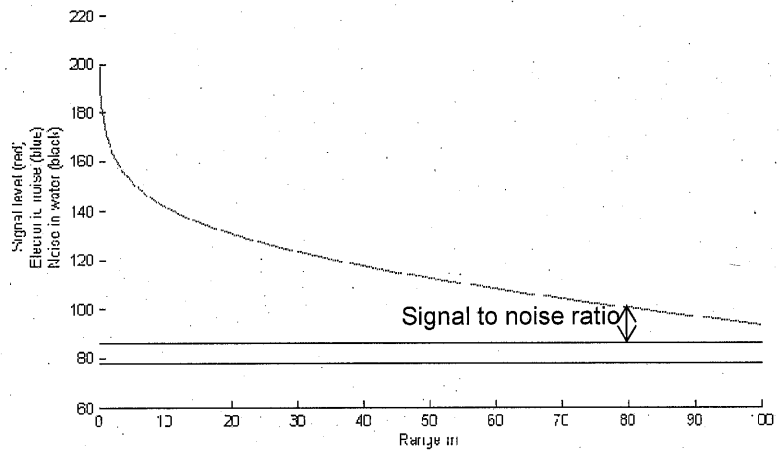

Fig.7: Signal-to-noise ratio

5.2 Contrast optimization

As we have seen earlier, the main parameter of the contrast is the distance between two successive hydrophones. A condition to optimize this contrast is to choose the angular distance of two successive ambiguous lobes in order to have an echographic contribution equal to the contribution of the secondary lobe in emission (figure).

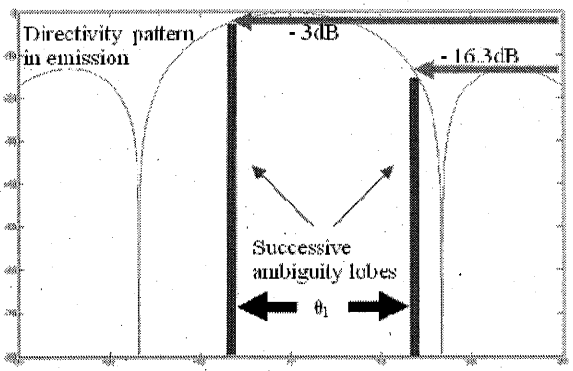

Fig.8: Condition of optimization of the distance between two sensors

This condition is respected for a distance between two hydrophones of: $di = 12.8mm$. With this condition the contrast in the gap is represented in the figure 9.

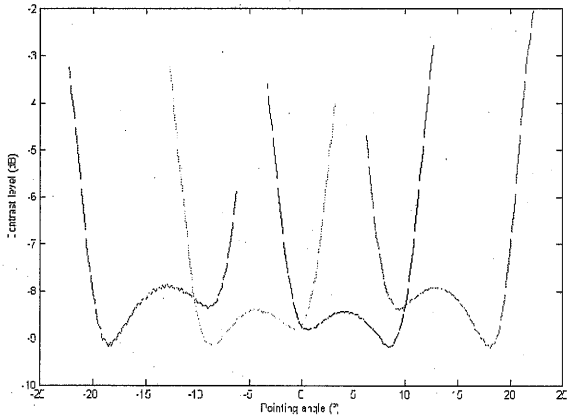

Fig.9: Contrast on the gap

This contrast can be improved with a Chebychev window in reception (around -11dB).

5.3 Resolutions

5.3.1 Range resolution

The bandwidth of our emitters is more than 40 kHz, and we work with the sectorized emission principle on four different frequencies near the central frequency. Thus the bandwidth for each sector is 10 kHz. The range resolution is: $\delta_r = \frac{c}{2B}\cos\theta$, where θ is the grazing angle. The range resolution is less than 10 centimeters in all the area of interest.

5.3.2 Across-track resolution

The across-track resolution is: $\delta_a = \frac{\lambda}{L}R$, with L the size of the reception antenna. With the optimized distance between two successive hydrophones seen earlier:

$$L = N_r * di = 48 * 12.8 = 614.4mm .$$

The range and across-track resolution, in the gap are:

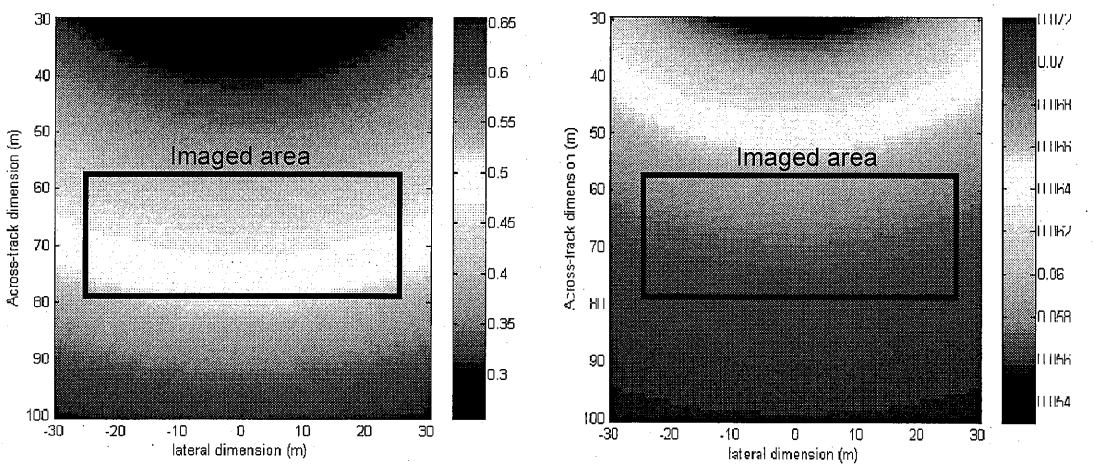

Across-track resolution Range resolution

Fig.10: Across-track and Range resolution

5.4 Physical dimension

The total system has a width of seventy centimeters and is implemented under the hull of Shadows (Fig.12).

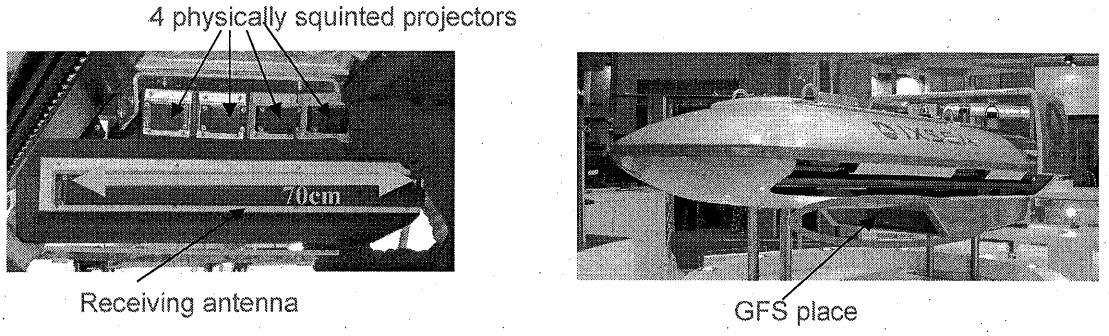

Fig.11: Implementation of the front-scan sonar

6 COHERENT SYNTHESIS

Making a coherent synthesis with front-scan sonar is equivalent to form a bidimensionnal network of sensors (figure 12).

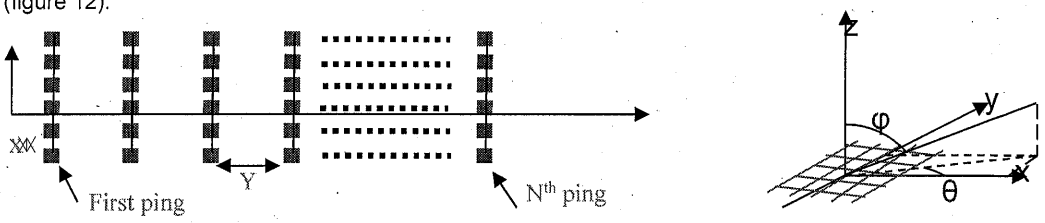

Fig.12: Problem geometry

The directivity of such an antenna is:

$$D(\theta,\varphi)=\frac{\sin\left(\frac{\pi N_x dx(\sin\varphi\cos\theta-\sin\varphi_0\cos\theta_0)}{\lambda}\right)\sin\left(\frac{\pi N_y dy(\sin\varphi\sin\theta-\sin\varphi_0\sin\theta_0)}{\lambda}\right)}{N_x N_y\sin\left(\frac{\pi dx(\sin\varphi\cos\theta-\sin\varphi_0\cos\theta_0)}{\lambda}\right)\sin\left(\frac{\pi dy(\sin\varphi\sin\theta-\sin\varphi_0\sin\theta_0)}{\lambda}\right)}$$

With our system and for a synthesis on ten pings, separated by one meter, the resolution in the gap for a range of seventy meters is improved:

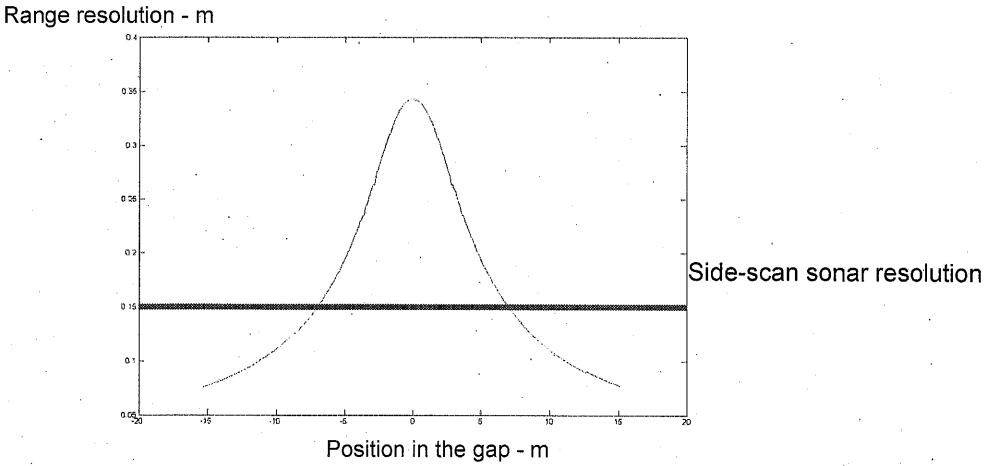

Fig.13: Theoretical resolution with synthesis

Nevertheless, other studies have to be made to confirm this possibility of process. Above all, the contrast along the track has to be determined.

7 CONCLUSION

The structure of our GapFiller has been designed. The sectorized emission principle enables to reach the imaging objectives with a small amount of data. An optimization of the contrast has been developed and the performances have been studied.
The across-track resolution is less than fifty centimeters in the entire gap.
Even if it is quite speculative yet, the possibility and the gain of the use of the coherent synthesis in the front-scan mode have been studied, and appears to be a hopeful method.

Tests at sea on the IXPLORER are planned during the summer of 2006 in La Ciotat bay.

Further works are also planned, like data fusing between each sector and with the side-scan sonar.

8 REFERENCES

1 F.Jean, "Shadows, a new synthetic aperture sonar system, by IXSEA SAS" *Oceans International 2006 proceedings.*
2 L.Kopp, "Etude GapFiller – éléments de spécification" *Technical note.*
3 R.J.Urick, "Principles of underwater sound" *Peninsula Publishing.*Los Altos, California.
4 X.Lurton, "Rappels et complements d'acoustiques sous-marine physique" *Technical note,* IFREMER-Centre de Brest.
5 R.E.François, G.R.Garrison, "Sound absorption based on ocean measurements" *JASA,* Vol72, N6, Dec 1982.
6 L.Camp, "Underwater transducers" *Wiley Interscience,* 1970, Chapter 6.
7 P.Caprais, "Towards a forward looking synthetic aperture sonar" *Sonar Signal Processing Conference 1998,* Institute of Acoustics, Weymouth - England.
8 P.Janvrin, "Sonar frontal pour l'imagerie par synthèse non-cohérente et la bathymétrie" *PHD thesis,*University of Paris 6 - France.